

TIME-DEPENDENT BEHAVIOR OF THERMAL HYDRAULIC PROPERTIES IN A TWO-CHANNEL BWR CORE MODEL

Doddy Y.F. Kastanya^{*}, Imelda Ariani^{**}

ABSTRACT

TIME-DEPENDENT BEHAVIOR OF THERMALHYDRAULIC PROPERTIES IN A TWO-CHANNEL BOILING WATER REACTOR CORE MODEL. A numerical model of a simplified boiling water reactor (BWR) core has been established by developing a Fortran code to perform the thermal hydraulic calculations. The core is modeled to consist of two channels connected at the upper and lower plenums. Prior to performing transient analysis, the code has been checked for its numerical stability. Two transients involving an increase in the inlet velocity and an increase in the heat generation rate have been examined. Numerical experiments of these transients exhibit the expected behaviors. Although the code, in its current state, is relatively simple in nature, it can be utilized as a foundation to develop more sophisticated core simulator code for thermal hydraulic analysis.

Keywords: core analysis, BWR, thermalhydraulics properties, numerical method.

ABSTRAK

PERILAKU PROPRTI TERMOHIDROLIKA SEBAGAI FUNGSI WAKTU DALAM MODEL TERAS REAKTOR AIR DIDIH DUA KANAL. Sebuah model numerik teras reaktor air didih sederhana telah dikembangkan dengan penulisan kode komputer dalam bahasa Fortran untuk perhitungan termo hidrolika. Model teras ini terdiri dari dua kanal yang dihubungkan oleh *plenum* atas dan bawah. Sebelum memanfaatkan program ini sebagai alat analisis, program tersebut telah terlebih dahulu diuji kestabilan numeriknya. Dua buah transien yang melibatkan kenaikan kecepatan aliran air ke dalam teras dan kenaikan panas dalam teras telah dipelajari. Hasil dari eksperimen-eksperimen numerik ini menunjukkan perilaku yang diharapkan. Kenyataan bahwa program komputer ini masih sederhana, tidak menutup kemungkinan bagi pengembangannya untuk menjadi suatu program simulasi termo hidrolika dari teras reaktor yang lebih canggih.

Kata kunci: Analisis Teras, Reaktor Air Didih, Properti Termohidrolika, Metoda Numerik.

^{*} Pusat Pendayagunaan Iptek Nuklir (PpdIN) – BATAN, e-mail: kastanya@batan.go.id

^{**} Pusat Pengembangan Sistem Reaktor Maju (P2SRM) – BATAN, e-mail: ariani@batan.go.id

INTRODUCTION

The purpose of this study is to develop a numerical model of a BWR core which can be utilized to analyze the distribution of various thermal-hydraulic properties in the core, *e.g.* pressure, density, and void fraction. Although a typical BWR core consists of hundreds of flow channels, *i.e.* fuel bundles, the representative model developed in this study has only two channels connected by the upper and lower plenums. Needless to say that while the pressure of the system in this model can be maintained at the typical value for a BWR, *i.e.* around 1000 psi, the mass flow rate into the core must be adjusted appropriately so that a realistic pressure drop across the core will still be observed.

The model developed in this study can be extended to include more flow channels and can even be incorporated into BWR core simulators like MICROBURN-B2 [1], PRESTO-B [2], FLARE [3], SIMULATE [4], and FORMOSA-B [5, 6, 7]. The model can also be utilized to perform other studies such that analyzing the behavior of various void-quality correlations, evaluating the effect of spacer grids on thermal hydraulic property distributions, or even evaluating the behavior of thermal hydraulics properties during certain accident scenarios, *e.g.* power excursion or LOCA.

A brief description of the problem statement and summarized derivations of the system of equations are presented in Section 2. Results from numerical experiments conducted using this code are summarized and analyzed in Section 3. Section 4 will provide a succinct conclusion from this study and offer some ideas for future research activities.

PROBLEM STATEMENT AND DERIVATION OF THE SYSTEM OF EQUATIONS

A simplistic representation of a BWR vessel is illustrated in Figure 1. The system is modeled as two channels connected at their inlets and outlets (the lower and upper plenums). Boundary conditions for this system consist of inlet velocity and exit pressure. In this study, the behavior of the transient solutions will be observed as a function of power (heat input) and velocity. It is assumed that the exit pressure is maintained constant at 1000 psi and there exists a 10 degree subcooling at the inlet.

For this model, it is assumed that a mixture drift flux model [8] is valid and given by the following expressions

Mixture Continuity

$$A_x \frac{\partial \mathbf{r}}{\partial t} + \frac{\partial}{\partial z} (\mathbf{r} v A_x) = 0 \quad (1)$$

Mixture Internal Energy

$$A_x \frac{\partial}{\partial t} (\mathbf{n} u) + \frac{\partial}{\partial z} (\mathbf{n} v A_x) = -P \frac{\partial}{\partial z} (v A_x) - P \frac{\partial}{\partial z} \left(\frac{\mathbf{a}_l \mathbf{r}_l \mathbf{a}_g \mathbf{r}_g}{\mathbf{r}} v_{fg} v_r A_x \right) - \frac{\partial}{\partial z} \left(\frac{\mathbf{a}_l \mathbf{r}_l \mathbf{a}_g \mathbf{r}_g}{\mathbf{r}} u_{fg} v_r A_x \right) + q' \quad (2)$$

Mixture Momentum

$$\mathbf{r} \frac{\partial v}{\partial t} + \mathbf{r} v \frac{\partial v}{\partial z} = -\frac{\partial P}{\partial z} - \frac{\partial}{\partial z} \left(\frac{\mathbf{a}_l \mathbf{r}_l \mathbf{a}_g \mathbf{r}_g}{\mathbf{r}} v_r^2 \right) - \mathbf{r} g \sin \mathbf{q} - \left(\frac{\mathbf{t}_w P_w}{A_x} \right)_{2f} \quad (3)$$

A state equation of the form $\mathbf{r} = \mathbf{r}(u, P)$ is utilized to obtain closure where both phases are required to be at equilibrium. The mixture variables \mathbf{r} , u , and v can be expressed in terms of phasic properties through the following definitions

$$\mathbf{r} = \mathbf{a}_l \mathbf{r}_l + \mathbf{a}_g \mathbf{r}_g \quad (4)$$

$$\mathbf{n} u = \mathbf{a}_l \mathbf{r}_l u_l + \mathbf{a}_g \mathbf{r}_g u_g \quad (5)$$

$$\mathbf{r} v = \mathbf{a}_l \mathbf{r}_l v_l + \mathbf{a}_g \mathbf{r}_g v_g \quad (6)$$

The relative velocity (v_r) is typically a correlated function depending on the flow regime. For this work, a bubbly flow regime is assumed and the relative velocity is given by

$$v_r = \frac{1.41}{\mathbf{a}_l} \left[\frac{\mathbf{a}_g (\mathbf{r}_l - \mathbf{r}_g)}{\mathbf{r}_l^2} \right]^{0.25} \quad (7)$$

For the temporal treatment, a semi-implicit time discretization is assumed, with the drift flux terms evaluated explicitly.

There are several types of node, each of which requires a particular treatment in deriving the finite difference analogs of the mixture and state equations. These treatments will be discussed in details in this paper using the regular nodes and node 1 (similar to node 13) as examples. The resulting system of equations will be algebraically reduced to just in term of pressures. However, in order to conserve space, the lengthy equation reduction process will not be presented in this paper.

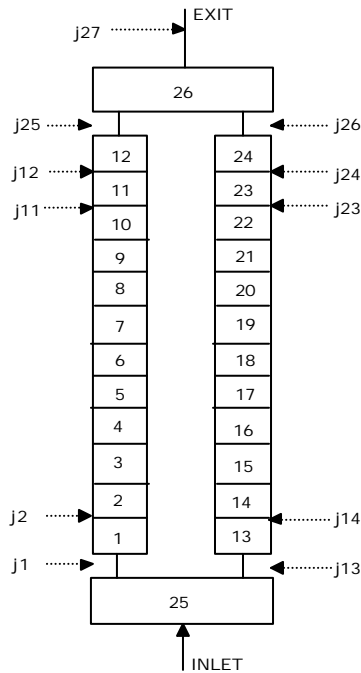


Figure 1. Diagram of nodalization scheme

Regular Nodes

The derivation for the regular nodes will be presented here. Nodes 2 through 11 and 14 through 23 are considered regular nodes (see Figure 1).

Mass Equation

$$A_{xj} \left\{ \frac{\mathbf{r}_j^{t+\Delta t} - \mathbf{r}_j^t}{\Delta t} \right\} + \left\{ \frac{\mathbf{r}_{j+1/2}^t v_{j+1/2}^{t+\Delta t} A_{xj} - \mathbf{r}_{j-1/2}^t v_{j-1/2}^{t+\Delta t} A_{xj-1}}{\Delta z} \right\} = 0 \quad (8)$$

Internal Energy Equation

$$\begin{aligned} A_{xj} \left\{ \frac{(\mathbf{r}u)_j^{t+\Delta t} - (\mathbf{r}u)_j^t}{\Delta t} \right\} + \left\{ \frac{(\mathbf{r}u)_{j+1/2}^t v_{j+1/2}^{t+\Delta t} A_{xj} - (\mathbf{r}u)_{j-1/2}^t v_{j-1/2}^{t+\Delta t} A_{xj-1}}{\Delta z} \right\} = \\ - C_1 P_j^t \left\{ \frac{v_{j+1/2}^{t+\Delta t} A_{xj} - v_{j-1/2}^{t+\Delta t} A_{xj-1}}{\Delta z} \right\} - \frac{C_1 P_j^t}{\Delta z} \left[\left(\frac{\mathbf{a}_l \mathbf{a}_g \mathbf{r}_l \mathbf{r}_g}{\mathbf{r}} v_{fg} v_r A_x \right)^t \right]_{j-1/2}^{j+1/2} \\ - \frac{1}{\Delta z} \left[\left(\frac{\mathbf{a}_l \mathbf{a}_g \mathbf{r}_l \mathbf{r}_g}{\mathbf{r}} u_{fg} v_r A_x \right)^t \right]_{j-1/2}^{j+1/2} + q' \end{aligned} \quad (9)$$

Momentum Equation

$$\begin{aligned} \mathbf{r}_{j+1/2}^t \left\{ \frac{v_{j+1/2}^{t+\Delta t} - v_{j+1/2}^t}{\Delta t} \right\} + \mathbf{r}_{j+1/2}^t v_{j+1/2}^t \left\{ \frac{v_{j+1/2}^t - v_{j-1/2}^t}{\Delta z} \right\} = -C_2 \left\{ \frac{P_{j+1}^{t+\Delta t} - P_j^{t+\Delta t}}{\Delta z} \right\} \\ - K_{j+1/2}^t \frac{\mathbf{r}_{j+1/2}^t}{2\Delta z} (2v_{j+1/2}^{t+\Delta t} - v_{j+1/2}^t) v_{j+1/2}^t - \mathbf{r}_{j+1/2}^t g - \frac{1}{\Delta z} \left\{ \left(\frac{\mathbf{a}_l \mathbf{a}_g \mathbf{r}_l \mathbf{r}_g}{\mathbf{r}} v_r^2 \right)^t \right\}_{j-1/2}^{j+1/2} \end{aligned} \quad (10)$$

Modified State Equation

$$\mathbf{r}_j^{t+\Delta t} = \tilde{\mathbf{r}}_j^t + \left((\mathbf{r}u)_j^{t+\Delta t} - \tilde{\mathbf{r}}_j^t u_j^t \right) \frac{\partial \mathbf{r}}{\partial (\mathbf{r}u)} \Big|_j^t + (P_j^{t+\Delta t} - P_j^t) \frac{\partial \mathbf{r}}{\partial P} \Big|_j^t \quad (11)$$

the $u_j^{t+\Delta t}$ term must be calculated such that the following equation holds:

$$\mathbf{r}_j^{t+\Delta t} = \tilde{\mathbf{r}}_j^t + \left(\mathbf{r}_j^{t+\Delta t} u_j^{t+\Delta t} - \tilde{\mathbf{r}}_j^t u_j^t \right) \frac{\partial \mathbf{r}}{\partial (\mathbf{r}u)} \Big|_j^t + \left(P_j^{t+\Delta t} - P_j^t \right) \frac{\partial \mathbf{r}}{\partial P} \Big|_j^t \quad (12)$$

The convergence on $\mathbf{r}u$ must satisfy:

$$\left| \frac{\mathbf{r}_j^{t+\Delta t} u_j^{t+\Delta t} - (\mathbf{r}u)_j^{t+\Delta t}}{(\mathbf{r}u)_j^{t+\Delta t}} \right| \leq \mathbf{e}_{ru}.$$

Nodes 1 And 13

Note that the equations for node 1 will be presented in this section.

Mass Equation

$$A_{x1} \left\{ \frac{\mathbf{r}_1^{t+\Delta t} - \mathbf{r}_1^t}{\Delta t} \right\} + \left\{ \frac{\mathbf{r}_{j2}^t v_{j2}^{t+\Delta t} A_{x1} - \mathbf{r}_{j1}^t v_{j1}^{t+\Delta t} A_{x1}}{\Delta z} \right\} = 0 \quad (13)$$

Internal Energy Equation

$$A_{x1} \left\{ \frac{(\mathbf{r}u)_1^{t+\Delta t} - (\mathbf{r}u)_1^t}{\Delta t} \right\} + \left\{ \frac{(\mathbf{r}u)_{j2}^t v_{j2}^{t+\Delta t} A_{x1} - (\mathbf{r}u)_{j1}^t v_{j1}^{t+\Delta t} A_{x25}}{\Delta z} \right\} =$$

$$\begin{aligned}
& -C_1 P_1^t \left\{ \frac{v_{j2}^{t+\Delta t} A_{x1} - v_{j1}^{t+\Delta t} A_{x25}}{\Delta z} \right\} - \frac{C_1 P_1^t}{\Delta z} \left[\left(\frac{\mathbf{a}_l \mathbf{a}_g \mathbf{r}_l \mathbf{r}_g}{\mathbf{r}} v_{fg} v_r A_x \right)^t \right]_{j1}^{j2} \\
& - \frac{1}{\Delta z} \left[\left(\frac{\mathbf{a}_l \mathbf{a}_g \mathbf{r}_l \mathbf{r}_g}{\mathbf{r}} u_{fg} v_r A_x \right)^t \right]_{j1}^{j2} + q'
\end{aligned} \tag{14}$$

Momentum Equation

(a) At Junction #2

$$\begin{aligned}
& \mathbf{r}'_{j2} \left\{ \frac{v_{j2}^{t+\Delta t} - v_{j2}^t}{\Delta t} \right\} + \mathbf{r}'_{j2} v_{j2}^t \left\{ \frac{v_{j2}^t - v_{j1}^t}{\Delta z} \right\} = -C_2 \left\{ \frac{P_2^{t+\Delta t} - P_1^{t+\Delta t}}{\Delta z} \right\} \\
& - K'_{j2} \frac{\mathbf{r}'_{j2}}{2\Delta z} (2v_{j2}^{t+\Delta t} - v_{j2}^t) |v_{j2}^t| - \mathbf{r}'_{j2} g - \frac{1}{\Delta z} \left\{ \left(\frac{\mathbf{a}_l \mathbf{a}_g \mathbf{r}_l \mathbf{r}_g}{\mathbf{r}} v_r^2 \right)^t \right\}_{j1}^{j2}
\end{aligned} \tag{15}$$

(b) At Junction #1

$$\begin{aligned}
& \mathbf{r}'_{j1} \left\{ \frac{v_{j1}^{t+\Delta t} - v_{j1}^t}{\Delta t} \right\} + \mathbf{r}'_{j1} v_{j1}^t \left\{ \frac{v_{j1}^t - v_{inlet}^t}{\Delta z} \right\} = -C_2 \left\{ \frac{P_1^{t+\Delta t} - P_{25}^{t+\Delta t}}{\Delta z} \right\} \\
& - K'_{j1} \frac{\mathbf{r}'_{j1}}{2\Delta z} (2v_{j1}^{t+\Delta t} - v_{j1}^t) |v_{j1}^t| - \mathbf{r}'_{j1} g - \frac{1}{\Delta z} \left\{ \left(\frac{\mathbf{a}_l \mathbf{a}_g \mathbf{r}_l \mathbf{r}_g}{\mathbf{r}} v_r^2 \right)^t \right\}_{inlet}^{j1}
\end{aligned} \tag{16}$$

Modified State Equation

$$\mathbf{r}'_1^{t+\Delta t} = \tilde{\mathbf{r}}'_1 + \left((\mathbf{ru})_1^{t+\Delta t} - \tilde{\mathbf{r}}'_1 u'_1 \right) \frac{\partial \mathbf{r}}{\partial (\mathbf{ru})} \Big|_1^t + (P_1^{t+\Delta t} - P_1^t) \frac{\partial \mathbf{r}}{\partial P} \Big|_1^t \tag{17}$$

RESULTS AND DISCUSSIONS

Before starting the discussion on several cases examined during this research, we would like to first examine the algorithm used in the code (see Figure 2). During the initialization process, it is assumed that there is no inlet flow and no heat addition to the channels. The initial pressure distribution is the hydrostatic pressure distribution. The node height (including the upper and lower plenums) is assumed to be uniform. The flow areas of the upper and lower plenums are twice as big as the channel flow area. The inlet and exit areas are half of the plenum areas.

After the initialization process, the coefficient matrix and the right hand side vector used for determining the new time pressure distribution are constructed. The derivation of the equations used for constructing the coefficient matrix and the right hand side vector are briefly outlined in the previous sections. The coefficient matrix can symbolically be written as follow:

$$\begin{bmatrix} T_{24 \times 24} & R_{24 \times 2} \\ B_{2 \times 24} & F_{2 \times 2} \end{bmatrix} \begin{bmatrix} (P_1)_{24 \times 1} \\ (P_2)_{2 \times 1} \end{bmatrix} = \begin{bmatrix} (S_1)_{24 \times 1} \\ (S_2)_{2 \times 1} \end{bmatrix} \quad (18)$$

where the subscripts (*e.g.*, 24x24) denote the size of the matrix (or vector). Since the diagonal blocks of this matrix structure are a tridiagonal matrix and a 2x2 matrix whose inverses are easy to be determined (*e.g.*, using the Thomas algorithm for the tridiagonal case and an analytic solution for the 2x2 matrix), the overall system of equation can be solved utilizing a substitution method in the following manner. First, the block system of equations can be rewritten as

$$TP_1 + RP_2 = S_1 \quad (19)$$

$$BP_1 + FP_2 = S_2 \quad (20)$$

Solve for P_1 using Eq. (19):

$$P_1 + T^{-1}RP_2 = T^{-1}S_1 \quad (21)$$

$$P_1 = T^{-1}S_1 - T^{-1}RP_2 \quad (22)$$

Substitute Eq. (22) into Eq. (20) and rearrange the resulting equation

$$B(T^{-1}S_1 - T^{-1}RP_2) + FP_2 = S_2 \quad (23)$$

$$(F - BT^{-1}R)P_2 = S_2 - BT^{-1}S_1 \quad (24)$$

P_2 can be solved by analytically finding the inverse of $F - BT^{-1}R$, which is a 2x2 matrix. P_1 can then be calculated by using Eq. (22).

After the pressure distribution is solved for the new time step, the resulting pressure should be checked as to whether they fall within the limits. If so, the next step can be performed which is to check the convergence of (\mathbf{ru}) . In order to determine the internal energy (u) for the new time step, a root finding method should be utilized. The following equation should hold:

$$\mathbf{r}_j^{t+\Delta t} = \mathbf{r}(u_j^{t+\Delta t}, P_j^{t+\Delta t}) \quad (25)$$

The root finding algorithm:

- 1) The non-linear equation to be solved is

$$F(u^{t+\Delta t}) = \mathbf{r}_j^{t+\Delta t} - \mathbf{r}(u_j^{t+\Delta t}, P_j^{t+\Delta t}) = 0$$

- 2) Start with a guess of $u^{t+\Delta t}$

- 3) Calculate $F(u^{t+\Delta t})$ and $\left. \frac{\partial F}{\partial u} \right|_{(u^{t+\Delta t}, P^{t+\Delta t})}$

- 4) New $u^{t+\Delta t}$ is determined by
$$u^{t+\Delta t} = u^{t+\Delta t} - \frac{F(u^{t+\Delta t})}{\left. \frac{\partial F}{\partial u} \right|_{(u^{t+\Delta t}, P^{t+\Delta t})}} .$$

- 5) Check convergence. If it does not converge, go to step (3) and repeat the process.

When Δt is sufficiently small, $u_j^{t+\Delta t}$ from solving Eq. (25) should also satisfy the following condition

$$(\mathbf{r}u)_j^{t+\Delta t} = \mathbf{r}(u_j^{t+\Delta t}, P_j^{t+\Delta t}) \times u_j^{t+\Delta t} \quad (26)$$

As indicated in Figure 2, once the new pressure distribution is within the acceptable range, the convergence of $(\mathbf{r}u)$ should be checked. This is a measure of the convergence or linearization error. If the convergence criteria is satisfied, the code will proceed to the next time step. The process is repeated until the desired length of time is reached.

The following subsections discuss and analyze results of several cases examined in this research (summarized in Table 1).

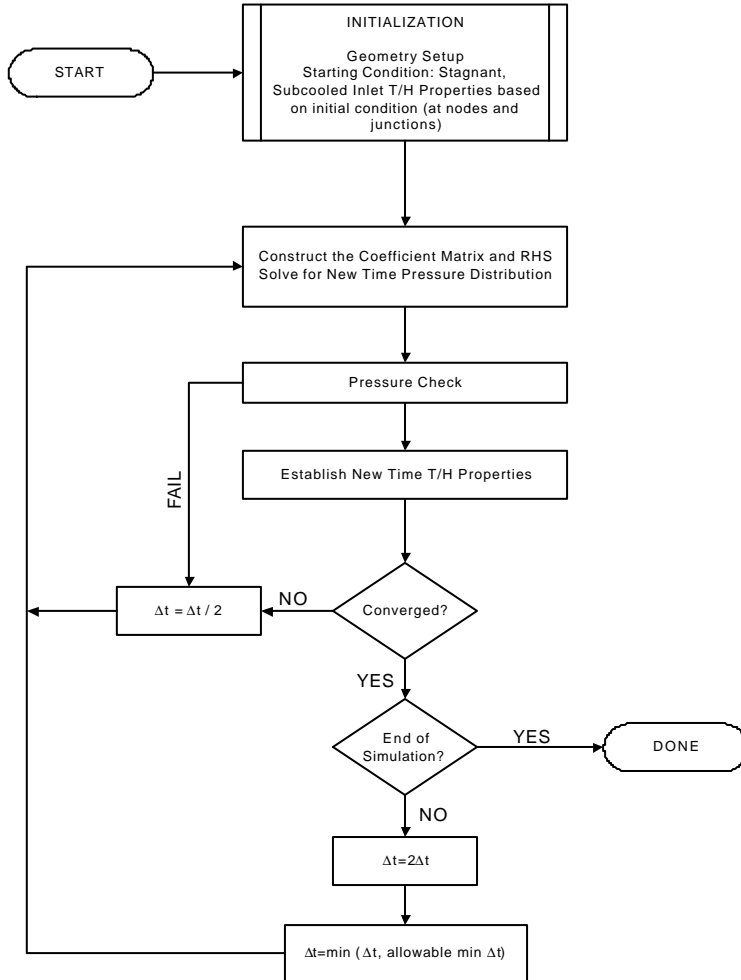


Figure 2. Flow chart of the algorithm

Table 1. Summary of Cases Examined

| Case | Description |
|----------|---|
| Case I | No heat and no inlet velocity are introduced into the system. |
| Case II | No heat is added into the system. Inlet velocity is gradually added (0.5 ft/sec is added every 5 seconds). |
| Case III | Inlet velocity is gradually introduced into the system. Heat addition is done at the rate of 1% of the total heat added into the system every minute. |

Case I: The Steady State Case

For this case, no heat addition and no inlet velocity are introduced into the system. The transient density and velocity can be observed in Figure 3 (a) and (b), respectively. From these two figures, one can see that steady state distributions have been established. The steady state check is a necessary process in validating the code. One should always check whether a program is numerically stable or not in the absence of external forces, in this case the additional heat or velocity. One needs to be cautious since numerical errors can be triggered not only by something physical related to the model but also by the numerical method itself, *e.g.* round-off errors. Unless the errors are indeed caused by the physical problem, a stable algorithm should be able to remove errors due to machine precisions.

Case II: Introduction Of Inlet Velocity

In the second case evaluated in this project, the inlet velocity is gradually increased by the rate of 0.5 ft/sec every 5 seconds. The introduction of inlet velocity changes the dynamics within the channel. While the change in velocity distribution should be obvious (see Figure 4), another thing to observe is the change in the pressure distribution up the channel. Note that while the transient was actually run for 5000 seconds (to ascertain that a new steady state condition is reached), only the results from the first 100 seconds are presented here in order to be able to observe the

changes. As clearly shown in Figure 5, with the introduction of inlet velocities, the inlet pressure and the pressure drop across the channel, as expected, increase.

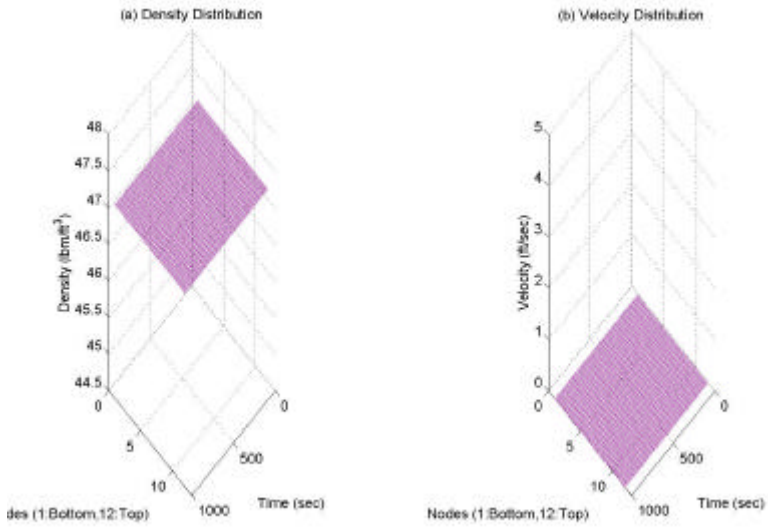


Figure 3. Density and velocity distribution for the steady state case

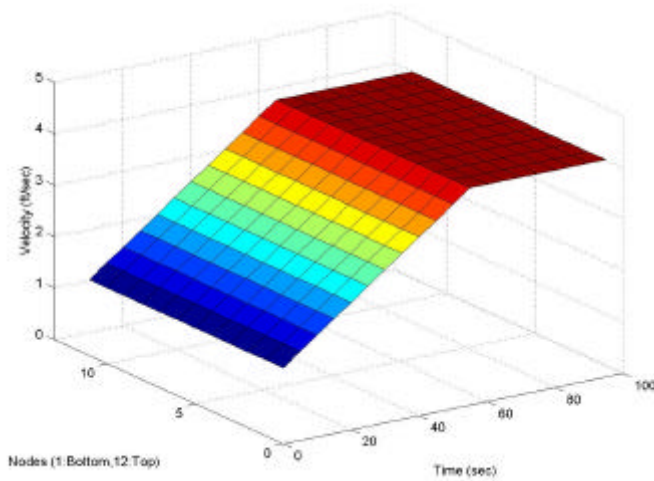


Figure 4. Velocity distribution for the gradual increase in velocity case

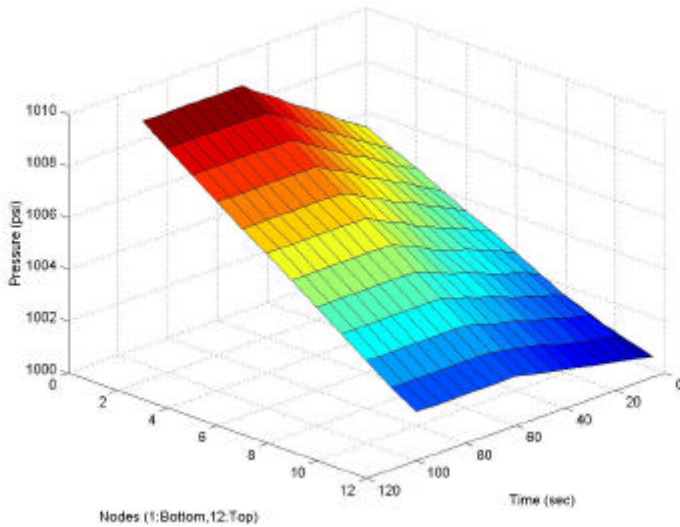


Figure 5. Pressure distribution for the gradual increase in velocity case

Case III: Velocity And Heat Addition

An additional external factor is added in this case. In addition to the introduction of inlet velocities as discussed in the previous sub-section, the heat factor is now taken into consideration. The heat is gradually added to both channels at the rate of 1% of the total rated power every minute, until the 25% of total rated power is reached. The transient is run for 5000 seconds to observe the changes not only during the heat addition process but also the new steady state condition afterward. Figure 6 and Figure 7 show the behavior of density and void fraction in the channel, respectively. From these figures, one can clearly see the reciprocal relationship between density and void fraction.

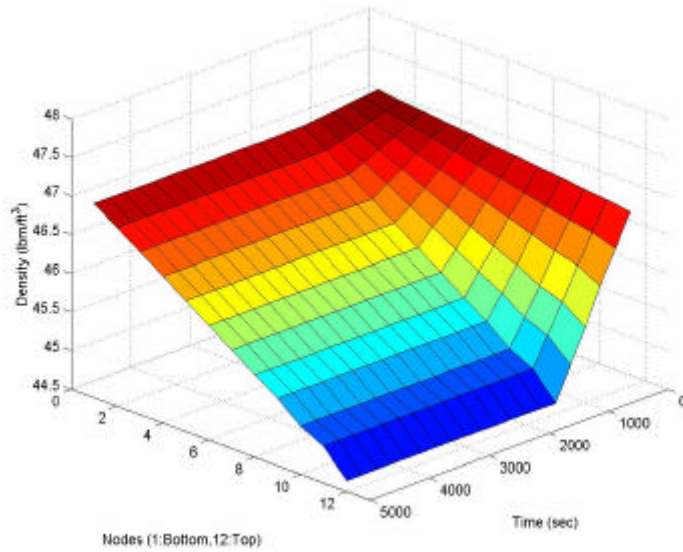


Figure 6. Density distribution for the increase in heat generation rate case

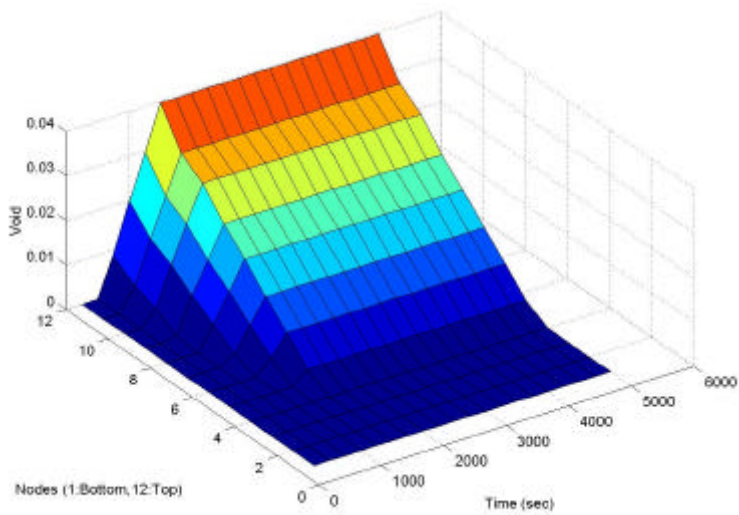


Figure 7. Void fraction distribution for the increase in heat generation rate case

As expected, as the heat is added into the coolant, the density of the coolant decreases and the presence of void fraction begins to be observed. From Figure 7, one can see that operating at 25% of the total rated power, the void fraction in the upper part of the channel is approximately 3%. In the full power operation of a typical BWR, the void fraction in this region can go up to around 60% to 70%.

CONCLUSIONS AND RECOMMENDATIONS

A numerical model, in the form of a Fortran code, of a simplified BWR core has been established. The core modeled consists of two flow channels. The thermal hydraulics properties of the coolant such as the density, void fraction, pressure, and velocity are monitored. A steady state simulation to validate the code has also been performed. Two transients involving an increase in inlet velocity and heat generation rate have been analyzed. Results from these numerical experiments behave as expected. Although this model, in its current state, is very simplistic in nature, it can serve as a foundation for developing a more sophisticated core analysis code. One simple and relatively straight forward modification toward realizing this goal is to include more flow channels in the model.

NOMENCLATURES

| | | | |
|--------|--|----------|-------------------------------------|
| A_x | : flow area (ft ²) | t | : time (sec) |
| ρ | : density (lbm/ft ³) | z | : elevation (ft) |
| u | : internal energy (BTU/lbm) | v | : velocity (ft/sec) |
| P | : pressure (psi) | α | : void fraction (unitless) |
| g | : gravity (32.2 ft/sec ²) | l | : [sub] saturated liquid state |
| g | : [sub] saturated vapor state | r | : [sub] relative |
| P_w | : Wetted perimeter (ft) | K | : local loss coefficient (unitless) |
| q' | : linear heat generation rate (BTU/ft.sec) | | |

REFERENCES

1. S. MISU and H. MOON, "SIEMENS 3D Steady State BWR Core Simulator MICROBURN-B2," *Proc. Intl. Conf. Nucl. Sci. and Tech.*, Vol. 2, p. 1097, Long Island, NY (1998).
2. S. BORRESEN, L. MOBERG, and J. RASMUSSEN, "Methods of PRESTO-B, A Three-Dimension BWR Core Simulation Code," Scandpower Inc. (1983).
3. D. L. DELP, D. L. FISHER, J. M. HARRIMAN, and M. J. STEDWELL, "FLARE, A Three-Dimensional Boiling Water Reactor Simulator," GEAP-4598, General Electric Co. (1964).
4. J. A. UMBARGER and A. S. di GIOVINE, *SIMULATE-3 Advanced Three-Dimensional Two-Group Reactor Analysis Code – User's Manual*, Studsvik Report SOA-95/15, Studsvik of America (1995).
5. B. R. MOORE, P. J. TURINSKY, and A. A. KARVE, "FORMOSA-B: A Boiling Water Reactor In-Core Fuel Management Optimization Package," *Nucl. Technol.*, **126**, 153 (1999).
6. A. A. KARVE and P. J. TURINSKY, "FORMOSA-B: A Boiling Water Reactor In-Core Fuel Management Optimization Package II," *Nucl. Technol.*, **131**, 48-68 (2000).
7. A. A. KARVE and P. J. TURINSKY, "FORMOSA-B: A Boiling Water Reactor In-Core Fuel Management Optimization Package III," *Nucl. Technol.*, **135**, 241-251 (2001).
8. N. E. TODREAS and M. S. KAZIMI, *Nuclear System I: Thermal Hydraulics Fundamentals*, Hemisphere Publishing Corporation, New York (1990).

DISKUSI

M. ARIFIN SANUSI

Apakah dengan penampilan tampilan grafik distribusi panas adalah hasil dari program yang dibuat itu?

DODDY KASTANYA

Grafik yang saya tampilkan diolah menggunakan software MATLAB. Software-software lainnya seperti EXCEL juga dapat digunakan. Sedangkan data yang digunakan untuk menggambar grafik-grafik tersebut dihasilkan oleh program komputer yang saya buat sendiri.

BAKRI ARBI

Rencana validasi dan benchmarking bagaimana? Ada baiknya kerjasama dengan Pusat Keselamatan Reaktor yang mempunyai beberapa loop-loop untuk simulasi.

DODDY KASTANYA

Tentunya saya sangat tertarik untuk mengecek program komputer yang saya buat dengan hasil eksperimen. Sehubungan dengan kerjasama yang mungkin dilakukan dengan P2TKN, saya berkeinginan untuk dapat menggabungkan RELAP yang kini dimiliki oleh P2TKN dengan suatu program komputer yang melakukan perhitungan neutronics

DAFTAR RIWAYAT HIDUP

1. Nama : Doddy Kastanya
2. Tempat/Tanggal Lahir : Jayapura, 28 February 1972
3. Instansi : BATAN
4. Pekerjaan / Jabatan :
5. Riwayat Pendidikan :
 - S1, North Carolina State University,USA
 - S2, North Carolina State University,USA
 - S3, North Carolina State University,USA
6. Pengalaman Kerja :
 - 2002-2003, Progress Energy Inc,Raleigh,USA.
 - 2004-Sekarang,PPdIN BATAN.
7. Organisasi Professional :
 - American Nuclear Society
 - Sigma XI Research Society
 - Alpha NU Sigma Nuclear Engineering Honor Society